

FIRST DETECTION OF DUST EMISSION IN A HIGH-VELOCITY CLOUD

M.-A. MIVILLE-DESCHÈNES¹ AND F. BOULANGER

Institut d'Astrophysique Spatiale, Université Paris-XI, 91405, Orsay Cedex, France

AND

W. T. REACH & A. NORIEGA-CRESPO

Spitzer Science Center, California Institute of Technology, MS 100-22, Pasadena, CA 91125, USA

Draft version February 5, 2008

ABSTRACT

By comparing sensitive Spitzer Space Telescope (SST) infrared and Green Bank Telescope 21 cm observations, we are able to report the first detection of dust emission in Complex C, the largest High Velocity Cloud in the sky. Dust in the region of Complex C studied here has a colder temperature ($T = 10.7^{+0.9}_{-0.8}$ K - 1σ) than the local interstellar medium ($T = 17.5$ K), in accordance with its great distance from the Galactic plane. Based on the metallicity measurements and assuming diffuse Galactic interstellar medium dust properties and dust/metals ratio, this detection could imply gas column densities more than 5 times higher than observed in HI. We suggest that the dust emission detected here comes from small molecular clumps, spatially correlated with the HI but with a low surface filling factor. Our findings imply that the HVCs' mass would be much larger than inferred from HI observations and that most of the gas falling on the Milky Way would be in cold and dense clumps rather than in a diffuse phase.

Subject headings: Galaxy: Halo, ISM: Clouds, ISM: Dust

1. INTRODUCTION

Since their discovery in HI observations (Muller et al. 1963), High Velocity Clouds (HVCs) have been the target of numerous studies (see van Woerden et al. (2004) for a thorough review) but nevertheless remain puzzling. It is now widely considered that many of them might be infalling clouds fueling the Galaxy with low metallicity gas. This hypothesis received strong support from ultraviolet observations showing that HVCs have a subsolar metallicity (Wakker et al. 1999) and a D/H ratio compatible with primordial abundances of deuterium (Sembach et al. 2004).

The present study focuses on the Spitzer Extra-Galactic First Look Survey (XFLS) field, a diffuse HI area ($N_{HI} \sim 2 \times 10^{20} \text{ cm}^{-2}$) at high Galactic latitude ($l = 88^\circ.3, b = 34^\circ.9$) programmed to study galaxy populations and clustering (Fang et al. 2004). The XFLS field is located on the edge of Complex C, a high-velocity gas structure spanning more than 1500 square degrees on the sky. Complex C has a subsolar metallicity ($\sim 0.1 - 0.3$) (Tripp et al. 2003), it contains ionised gas observed in $H\alpha$ emission (Tufte et al. 1998) and O VI absorption (Sembach et al. 2003) and is located at a distance greater than 5 kpc from the sun (Wakker 2001). Dust emission has been unsuccessfully looked for in HVCs using IRAS data (Wakker & Boulanger 1986). Upper limits were found to be compatible with their low HI column densities, low metallicity (and therefore low dust/gas ratio) and their large distance (i.e. fainter radiation field). In this study we revisit the dust/gas correlation in HVCs using new infrared and HI data.

2. DATA

¹ Senior Research Associate, Canadian Institute for Theoretical Astrophysics, University of Toronto, 60 St-George st, Toronto, Canada

In this study we used Spitzer Space Telescope (SST) MIPS 24 and 160 μm data of the XFLS. The field was covered by MIPS in 8 scan maps that were combined and destriped, then regridded to 16'' pixels and median-smoothed. We complemented the SST data with improved IRAS 60 and 100 μm maps (IRIS - Miville-Deschenes & Lagache (2005)). The FWHM angular resolution of the IRIS maps is $\sim 4'$ with a pixel size of 1'.5. The calibration uncertainties on diffuse emission of the SST and IRIS maps is 10 %. Bright point sources were removed from all infrared maps (SST and IRIS) before convolution by a Gaussian beam to bring all of them to the Green Bank Telescope (GBT) 9'.2 FWHM resolution. Fig. 1 shows the convolved maps.

The HI (21 cm) data we used in this study were obtained with the GBT, previously published and kindly made available by Lockman & Condon (2005). These observations cover a $3^\circ \times 3^\circ$ area centered at (J2000) $\alpha = 17^\text{h}18^\text{m}$, $\delta = +59^\circ30'$, which encloses the SST observations. The GBT data were corrected for stray-radiation contamination. The sampling was done at 1', the FWHM beam is 9.2', the channel width is $dv = 0.51 \text{ km s}^{-1}$ and the noise level in a single channel is 0.05 K.

3. HI DECOMPOSITION

Fig. 2 presents the average 21 cm spectrum of the field and two typical lines-of-sight. In addition to Complex C, the XFLS 21 cm data revealed two Intermediate-Velocity Clouds (IVC1 and IVC2) and a local component typical of high-latitude HI emission with a narrow cold component superimposed on a broad warm component (Lockman & Condon 2005). In this section we estimate the column density of each of these HI components. The HVC is well isolated in velocity space and its integrated emission was computed by adding all the channels where $-210 < v < -132 \text{ km s}^{-1}$. On the other hand the two IVCs and the local component overlap in

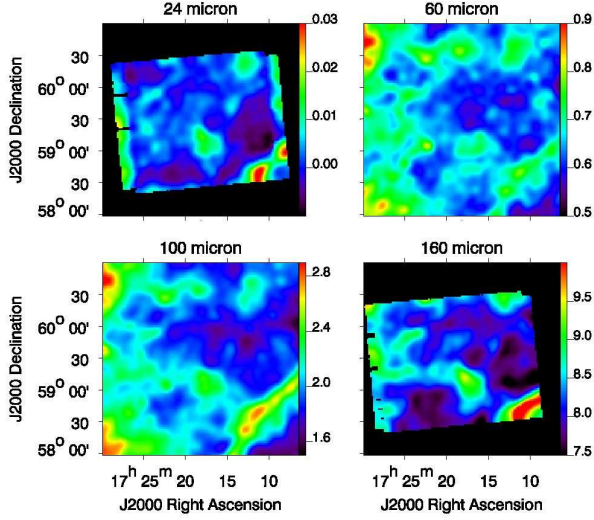


FIG. 1.— Infrared maps of the XFLS field at 24 and 160 micron from Spitzer and 60 and 100 micron from IRIS. All maps were convolved by a Gaussian beam to bring them to the GBT 9.2' FWHM resolution.

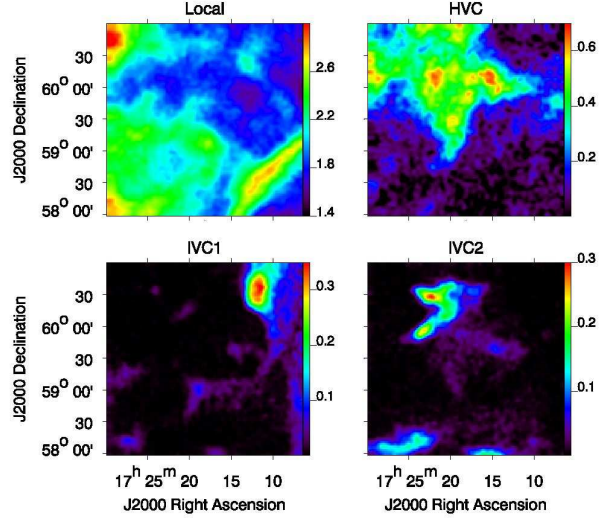


FIG. 3.— HI column density of the four HI components (Local, HVC, IVC1 and IVC2). All maps are in units of 10^{20} cm^{-2} . An opacity correction was applied to convert the 21 cm integrated emission to HI column density - see text for details.

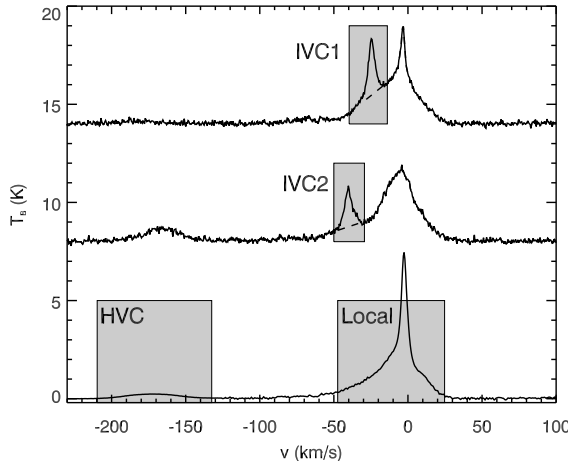


FIG. 2.— Decomposition of the 21 cm data. The bottom curve shows the 21 cm spectrum averaged over the whole field. The middle and top curves (shifted for clarity) are representative 21 cm spectra where the IVC1 (top) and IVC2 (middle) components are observed. The shaded rectangles indicate the velocity range used to extract the HI components.

velocity. The integrated emission of the two IVC components were computed by adding all the channels between $-40 < v < -14 \text{ km s}^{-1}$ for IVC1 and $-50 < v < -29 \text{ km s}^{-1}$ for IVC2 from which we subtracted the local component contribution estimated by interpolating a baseline on each spectrum (see Fig. 2). The local component's integrated emission was computed by adding all channels between $-48 < v < +25 \text{ km s}^{-1}$ from which the two IVC contributions were removed. There is still contribution from the local components in a few channels at $v < -48 \text{ km s}^{-1}$ but they were not added, as the emission is very diffuse and its structure within the noise.

In the optically-thin case (i.e. when the 21 cm bright-

ness temperature is much smaller than the HI kinetic temperature), the 21 cm integrated emission is proportional to the HI column density: $N_{HI}(x, y) = 1.823 \times 10^{18} \sum_v T_B(x, y, v) dv$. The local component is dominated by a broad (i.e. warm and optically-thin) component but a fraction of the emission comes from cold gas (narrow features) that needs to be corrected for opacity to properly estimate the column density. To do so we estimated the fraction of warm and cold gas on each line-of-sight using a Gaussian decomposition of each spectrum. For each Gaussian component we estimated its opacity correction, considering that thermal and turbulence broadening equally contribute to the velocity dispersion σ_v (i.e. spin temperature is $T_s = 121\sigma_v^2/2$), instead of the usual isothermal assumption (Lockman & Condon (2005) used $T_s = 80 \text{ K}$). This allowed us to compute a larger correction for the narrow than for the broad components. Overall the opacity correction for the local component is lower than 6 %. It reaches its maximum value in the bright filament (south-western part of the field, see Fig. 3) where our estimate of the HI kinetic temperature gets as low as 50 K. The opacity correction for the two IVCs and the HVC is less than 1% in accordance with their broad lines ($\text{FWHM} > 8 \text{ km s}^{-1}$). Fig. 3 presents the HI column density maps of the four HI components.

4. INFRARED-HI CORRELATION

The main goal of this study was to separate and determine the infrared emission of the HI components identified with the 21 cm observations. To do so we considered that the infrared map $I_\lambda(x, y)$ at wavelength λ can be represented by the following model

$$I_\lambda(x, y) = \sum_i \alpha_\lambda^i N_{HI}^i(x, y) + C_\lambda(x, y) \quad (1)$$

where $N_{HI}^i(x, y)$ is the column density of the i^{th} HI component, α_λ^i is the infrared-HI correlation coefficient of

component i at wavelength λ and $C_\lambda(x, y)$ is a residual term.

To estimate the correlation coefficients α_λ^i we performed a chi-square minimisation on the HI and infrared data based on the model given by Eq. 1. The infrared-HI correlation coefficients are collected in Table 1 and shown in Fig. 4. The standard deviation of the residual maps $C_\lambda(x, y)$ are also given in Table 1.

The uncertainties on α_λ^i given in Table 1 include calibration and statistical uncertainties, taking into account the data sampling. To estimate the impact of our opacity correction we made the same analysis with optically-thin HI maps and obtained the same results within the uncertainties.

The infrared-HI correlation presented here shows that the model used (Eq. 1) for the infrared emission is satisfying. At each wavelength the standard deviation of the residual term $C_\lambda(x, y)$ is in good concordance with the expected (Lagache et al. 2003) and measured (Miville-Deschénes et al. 2002) levels of the Cosmic Infrared Background (CIB) fluctuations (see Table 1), except at 160 μm where we report a significant residual excess. As the residues at 60 and 100 μm are in accordance with the CIB level, this analysis also leads us to conclude that dust associated with the Warm Ionised Medium (WIM) (Lagache et al. 1999) does not significantly bias our decomposition of the infrared emission in this field.

The striking result of this analysis is certainly the significant detection of the infrared emission associated with an HVC at all wavelengths. Our result at 100 μm is compatible with the upper limit given by Lockman & Condon (2005).

5. DUST PROPERTIES OF COMPLEX C

Using the infrared-HI correlation coefficients we now want to put contrains on the properties of the dust, especially in the HVC.

We assume that the emission from big grains at thermal equilibrium with the radiation field is a modified black body :

$$I_\lambda = \tau_\lambda B_\nu(T_{BG}) \quad (2)$$

where B_ν is the Planck function, T_{BG} is the big grains' equilibrium temperature and τ_λ the opacity, often expressed as $\tau_\lambda = N_{HI}\epsilon_\lambda$ where ϵ_λ is the dust emissivity per H atom. The emissivity is generally described as a power law : $\epsilon_\lambda = \epsilon_0\lambda^{-\beta}$ where β is the emissivity spectral index. Based on FIRAS data, Boulanger et al. (1996) give the following expression for the big grains' emissivity law in the local interstellar medium:

$$\epsilon_\lambda = 1.0 \times 10^{-25}(\lambda/250\mu\text{m})^{-2} \text{ cm}^2. \quad (3)$$

In this scheme, and at wavelengths where the emission is dominated by big grains, the infrared-HI correlation coefficients can be expressed as $\alpha_\lambda = \epsilon_\lambda B_\nu(T_{BG})$. Assuming that Very Small Grains (VSGs) do not contribute significantly in the far-infrared and taking $\beta = 2$ (Draine & Lee 1984; Boulanger et al. 1996), we use the 100 and 160 μm infrared-HI correlation coefficients to estimate the big grains' temperature T_{BG}^i of each HI component

$$\frac{\alpha_{100}^i}{\alpha_{160}^i} = \frac{B_\nu(100\mu\text{m}, T_{BG}^i)160^2}{B_\nu(160\mu\text{m}, T_{BG}^i)100^2} \quad (4)$$

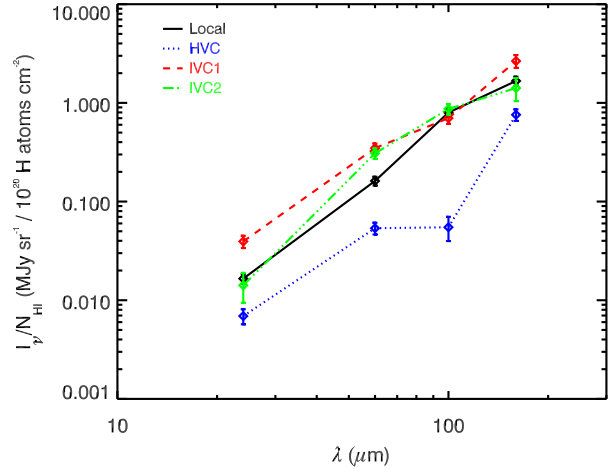


FIG. 4.— HI -infrared correlation coefficients for the Local, HVC, IVC1 and IVC2 components shown in Fig. 3. See Table 1 for details.

and the dust emissivities at 160 μm : $\epsilon_{160}^i = \alpha_{160}^i / B_\nu(160\mu\text{m}, T_{BG}^i)$. The big grain temperature and the 160 μm emissivity of each HI component are given in Table 2. In this table are also given the corresponding 1 and 3σ ranges on T_{BG}^i and ϵ_{160}^i computed using 1 and 3σ uncertainties on α_{100}^i and α_{160}^i .

6. DISCUSSION

The values of $T_{BG}^{local} = 17.4^{+1.4}_{-1.1}$ and $\epsilon_{160}^{local} = 3.0^{+1.9}_{-1.1} \times 10^{-25} \text{ cm}^2$ per H atom found for the local component are in very good agreement (within 1σ uncertainties) with the average values found for the Solar neighborhood by Boulanger et al. (1996) using COBE data : $T_{BG}^{soln} = 17.5$ K and $\epsilon_{160}^{soln} = 2.4 \times 10^{-25} \text{ cm}^2$ per H atom. This is an important validation of the photometric accuracy of the SST-MIPS data. On the other hand dust in the HVC is found to be significantly colder than in the local interstellar medium, even at the 3σ limit ($T_{BG}^{HVC} = 10.7^{+2.9}_{-3.0}$), which is consistent with a lower radiation field than in the Solar neighborhood due to its distance to the Galaxy (Wakker & Boulanger 1986). In addition we report an emissivity ϵ_{160} higher in the HVC than in the local ISM (see Table 2). An eventual contribution of VSGs to the far-infrared emission would have the effect of lowering T_{BG} and increasing ϵ_{160} even more.

For dust properties typical of the local interstellar medium, ϵ_λ should be proportional to the dust-to-gas mass ratio which, for standard metal depletion on grains, would scale with the metallicity. The fact that $\epsilon_{160}^{HVC} / \epsilon_{160}^{soln} > 1.6$ (3σ) is greater than the metallicity in Complex C ($Z_{HVC}/Z_\odot = 0.2 \pm 0.1$ according to Tripp et al. (2003)) could indicate a dust (and therefore gas) column density in Complex C more than 5 times larger than given by the HI emission.

Could it be dust associated with ionised gas ? H α and other ionised atomic lines have been detected in several HVCs. It is expected to come from a photoionized layer at the surface of the clouds which plunge into the Galactic halo. The column density of such a layer is $2 - 4 \times 10^{19} \text{ cm}^{-2}$ in Complex C (Wakker et al. 1999) which is similar to the HI column density in the HVC

TABLE 1
INFRARED-HI CORRELATION

| λ (μm) | α_{λ}^{Local} | α_{λ}^{HVC} | α_{λ}^{IVC1} | α_{λ}^{IVC2} | $\sigma(\text{Residue})$ (MJy sr^{-1}) | CIB estimate (MJy sr^{-1}) |
|--------------------------------|----------------------------|--------------------------|---------------------------|---------------------------|--|--|
| 24 | 0.017 ± 0.002 | 0.007 ± 0.002 | 0.039 ± 0.006 | 0.014 ± 0.005 | 0.004 | 0.004 |
| 60 | 0.16 ± 0.02 | 0.05 ± 0.01 | 0.35 ± 0.04 | 0.31 ± 0.04 | 0.03 | 0.02 |
| 100 | 0.80 ± 0.08 | 0.055 ± 0.015 | 0.70 ± 0.09 | 0.9 ± 0.1 | 0.09 | 0.07 |
| 160 | 1.7 ± 0.2 | 0.8 ± 0.1 | 2.7 ± 0.4 | 1.4 ± 0.4 | 0.30 | 0.11 |

Infrared-HI correlation coefficients (α_{λ}^i) given in MJy sr^{-1} (10^{20} H atoms) $^{-1}$ cm^2 for the four HI components (Local, HVC, IVC1 and IVC2) at 24, 60, 100 and 160 μm . The uncertainties on each α_{λ}^i is the 1σ uncertainty taking into account the statistical variance and instrumental uncertainties. Column 6 gives the standard deviation of the residual map and Column 7 is an estimate of the Cosmic Infrared Background (CIB) fluctuations based on the model of Lagache et al. (2003).

TABLE 2
DUST PARAMETERS

| | T_{BG} | 1σ | 3σ | ϵ_{160} | 1σ | 3σ |
|-------|----------|-----------|------------|------------------|-----------|------------|
| Local | 17.4 | 16.3-18.8 | 14.3-22.6 | 3.0 | 1.9-4.9 | 0.60-12.5 |
| HVC | 10.7 | 9.9-11.6 | 7.7-13.6 | 36.0 | 16.8-83.7 | 3.8-1442.8 |
| IVC1 | 14.6 | 13.6-15.8 | 11.8-19.4 | 13.2 | 7.0-24.1 | 1.6-79.6 |
| IVC2 | 19.4 | 17.1-23.1 | 14.1-107.4 | 1.5 | 0.5-3.6 | 0.003-15.5 |

Big Grain temperature (T_{BG} , given in Kelvin) and dust emissivity at 160 μm ($\epsilon_{160} = \tau_{160}/N_{HI}$ given in 10^{-25} cm^2 per H atom) and their corresponding 1 and 3 σ ranges for each HI component. The values for the local interstellar medium deduced from the COBE data (Boulanger et al. 1996) are $T_{BG} = 17.5$ K and $\epsilon_{160} = 2.4 \times 10^{-25}$ cm^2 .

seen in XFLS and therefore not enough to explain the high infrared emissivity measured here. In addition only the ionised gas spatially correlated with the HI would contribute to the infrared emissivity. Could it be dust associated with diffuse H₂? Two detections of H₂ in absorption with FUSE have been reported but the column densities are much lower than those of HI (Richter et al. 2001a). Other attempts have been unsuccesful; CO was not found in emission (Wakker et al. 1997) nor HCO⁺ in absorption (Combes & Charmandaris 2000). Furthermore abundance measurements in HVCs show no sign of iron depletion (Murphy et al. 2000; Tripp et al. 2003) which has been used as a strong argument in favor of very low dust in HVCs.

To reconcile our findings with previous work we suggest that HVCs could be multiphase gas including small and dense molecular clumps with a low surface filling factor (and therefore undetected with pencil beam absorption observations) bathing in a diffuse phase seen in absorption. The dust emission reported here would mainly originate in these clumps, spatially correlated with HI, which would have a larger iron depletion than

in the diffuse phase of HVCs. Evidence of the existence of such small molecular clumps was found in cirrus clouds (Heithausen 2004) and in the Magellanic Stream (Sembach et al. 2001). Additional observations of HVCs with the Spitzer Space Telescope are needed to confirm our result.

If our result reveals a general property of HVCs, it would mean that their mass is much larger than what can be inferred from HI observations and that most of the gas is in a dense phase. An infall of 1 M_{\odot} /year is needed to explain the star formation rate, the distribution of stellar metallicities with age and the presence of a bar in the Milky Way and in other galaxies. The current idea is that this infalling gas is diffuse (ionised and neutral) resulting from the cooling of very hot halo gas. Our result changes this picture by showing that most of the infalling gas is in dense and cold clumps, leaving open the question of the origin and stability of such structures.

HVCs typically contribute to $< 10\%$ of the HI column density at high latitude, but with its temperature lower than in the local interstellar medium, dust in HVCs could contribute a much larger fraction to the sub-millimeter and millimeter emission. Observations in this wavelength range, with Herschel and Planck for instance, could be used as a tracer of the column density of HVCs and as a distance indicator, using the dust temperature to put constraints on the radiation field strength. If the detection presented in this study is confirmed and is typical of HVCs, it could also have a strong impact on the analysis of observational cosmology data (e.g. WMAP, Planck) that do not to this day take this foreground component into account.

The authors thank the anonymous referee for a careful reading of the manuscript and very helpful comments. M.A.M.D. acknowledges support from The Canadian Space Agency. This research has made use of NASA's Astrophysics Data System Bibliographic Services.

REFERENCES

- Boulanger, F., et al. 1996, A&A, 312, 256.
 Combes, F. & Charmandaris, V. 2000, A&A, 357, 75.
 Draine, B. T. & Lee, H. M. 1984, ApJ, 285, 89.
 Fang, F. et al. 2004, ApJS, 154, 35.
 Heithausen, A. 2004, ApJ, 606, L13.
 Lagache, G., Abergel, A., Boulanger, F., Desert, F. X., Puget, J. L. 1999, A&A, 344, 322.
 Lagache, G., Dole, H. & Puget, J. L. 2003, MNRAS, 338, 555.
 Lockman, F. J. & Condon, J. J. 2005, AJ, 129, 1968.
 Miville-Deschenes, M.-A. & Lagache, G. 2005, ApJS, 157, 302.
 Miville-Deschênes, M. A., Lagache, G., & Puget, J.-L.. 2002, A&A, 393, 749.
 Muller, C. A., Oort, J. H. & Raimond, E. 1963, Comptes rendus de l'Académie des Sciences de Paris, 257, 1661.
 Murphy, E. M., et al. 2000, ApJ, 538, L35.
 Richter, P., Sembach, K. R., Wakker, B. P. & Savage, B. D. 2001a, ApJ, 562, L181.
 Richter, P., et al. 2001b, ApJ, 559, 318.
 Sembach, K. R., Howk, J. C., Savage, B. D., & Shull, J. M. 2001, AJ, 121, 992.
 Sembach, K. R. et al. 2003, ApJS, 146, 165.

- Sembach, K. R. et al. 2004, ApJS, 150, 387.
- Tripp, T. M. et al. 2003, AJ, 125, 3122.
- Tufte, S. L., Reynolds, R. J. & Haffner, L. M. 1998, ApJ, 504, 773.
- van Woerden, H., Wakker, B. P., Schwarz, U. J. & De Boer, K. S. 2004, *High Velocity Clouds*. Kluwer Academic Publishers, Dordrecht.
- Wakker, B. P. & Boulanger, F. 1986, A&A, 170, 84.
- Wakker, B. P., Murphy, E. M., van Woerden, H. & Dame, T. M. 1997, ApJ, 488, 216.
- Wakker, B. P. et al. 1999, Nature, 402, 388.
- Wakker, B. P. 2001, ApJS, 136, 463.